

Figure S3.1. Heatmap of 214 genes differentially expressed following injection with LPS. Scale is log2-fold change, with lower expression in purple and higher expression in dark orange.

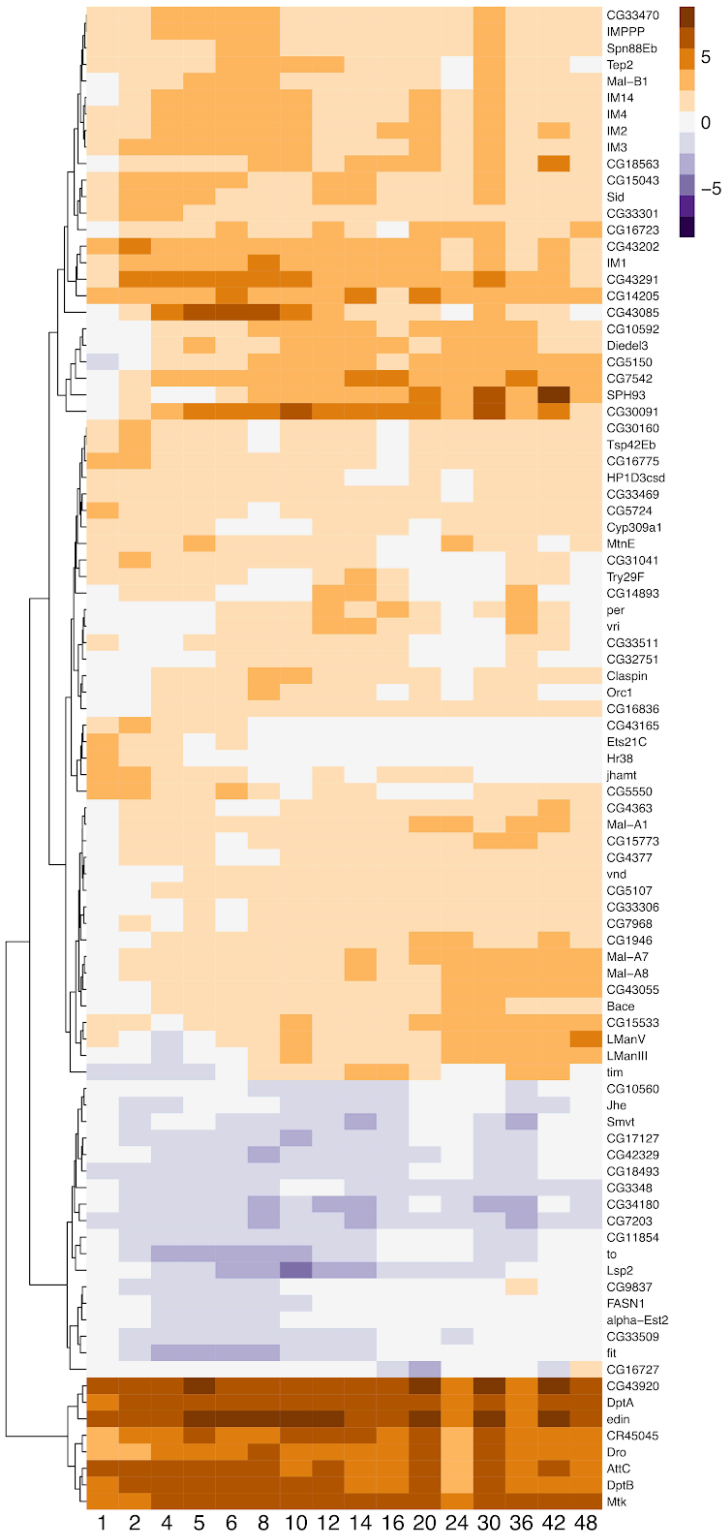


Figure S3.2. GC edge between *period* and *takeout*. Windows in which a significant Granger Causal relationship is established are colored in blue and are contained in a dashed blue box marking the plot area, non-significant windows are grey below the plot.

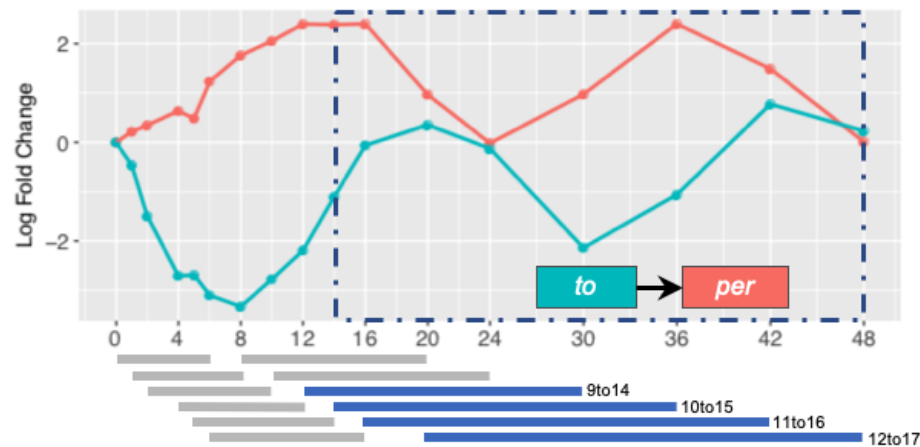


Figure S3.3. GC edge between *Smt* and *takeout*. Windows in which a significant Granger Causal relationship is established are colored in blue and are contained in a dashed blue box marking the plot area, non-significant windows are grey below the plot.

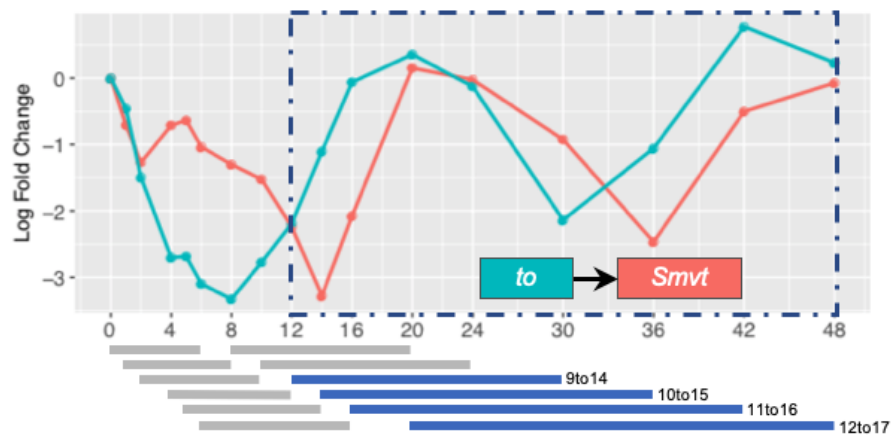


Figure S3.4. GC filtered network. The network was pruned to only the edges with at least three consecutive windows of GC significance, have a negative GC relationship, and excludes genes identified with JTK_Cycle.

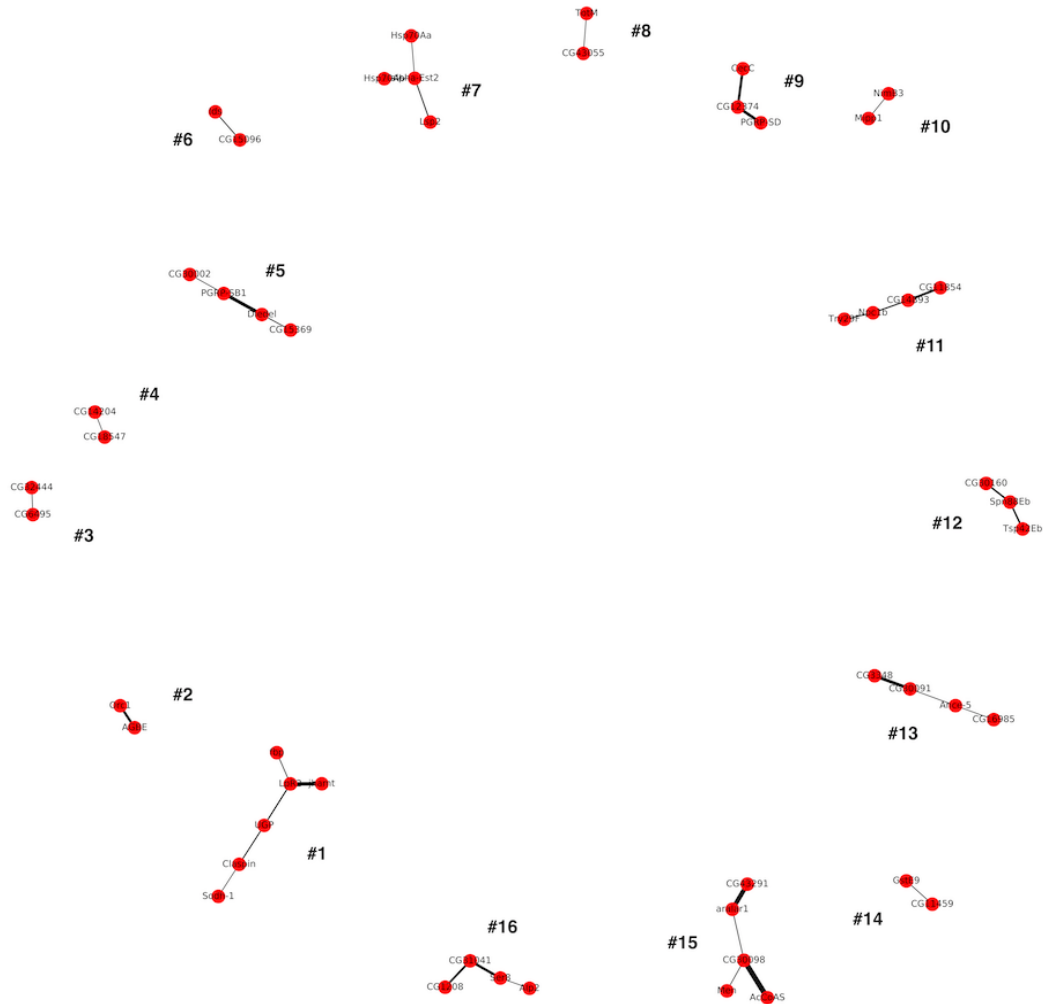


Figure S3.5. GC edge between *Claspin* and *UGP*. Windows in which a significant Granger Causal relationship is established are colored in blue and are contained in a dashed blue box marking the plot area, non-significant windows are grey below the plot.

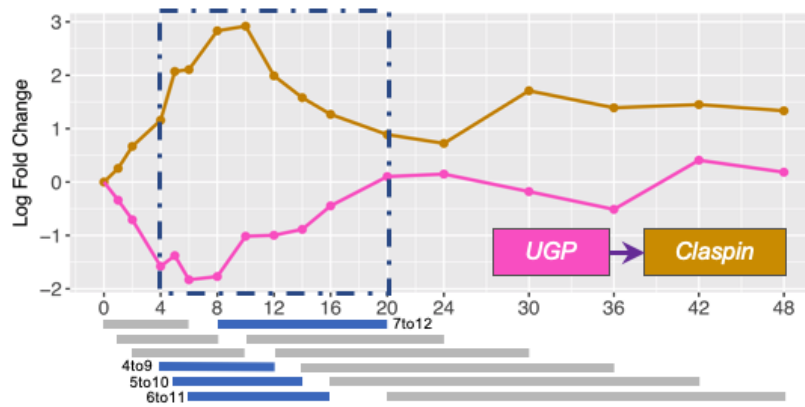


Figure S3.6. GC edge between *LpR2* and *fbp*. Windows in which a significant Granger Causal relationship is established are colored in blue and are contained in a dashed blue box marking the plot area, non-significant windows are grey below the plot.

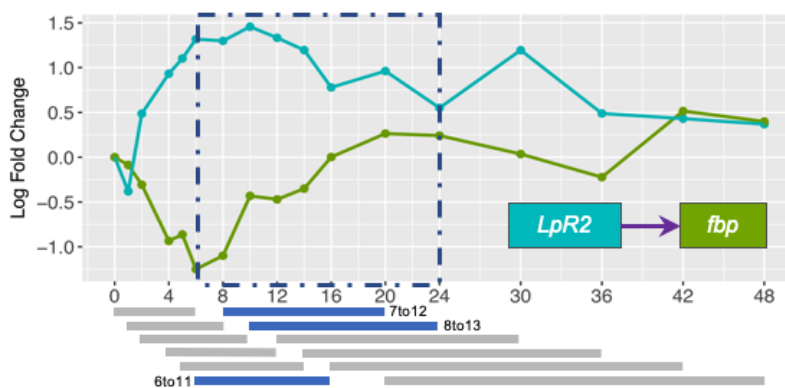


Figure S3.7. Down-regulated pathway corresponding to ‘mitotic DNA replication checkpoint’

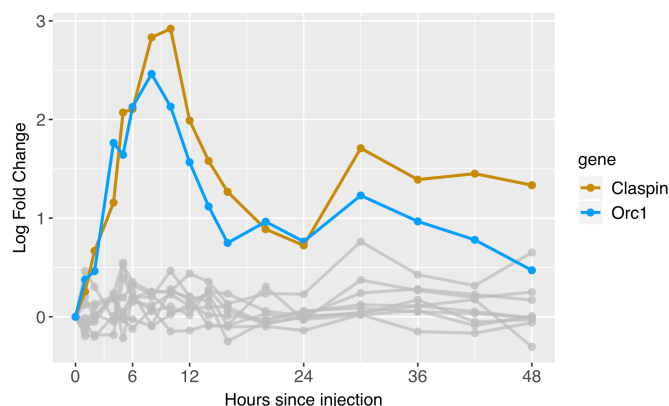
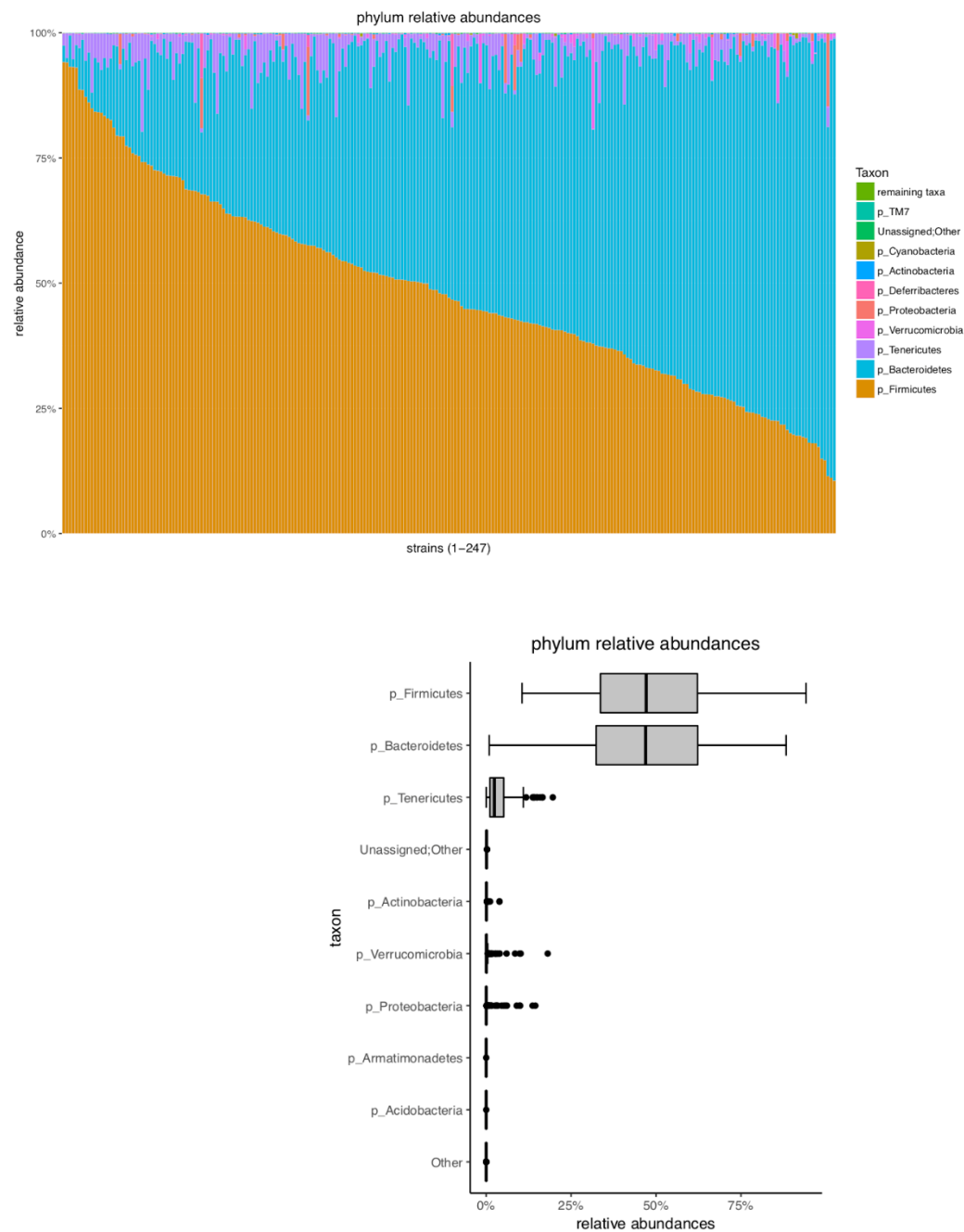
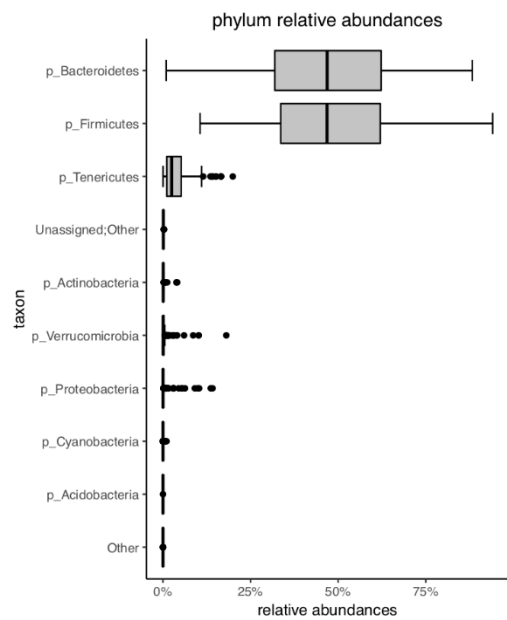
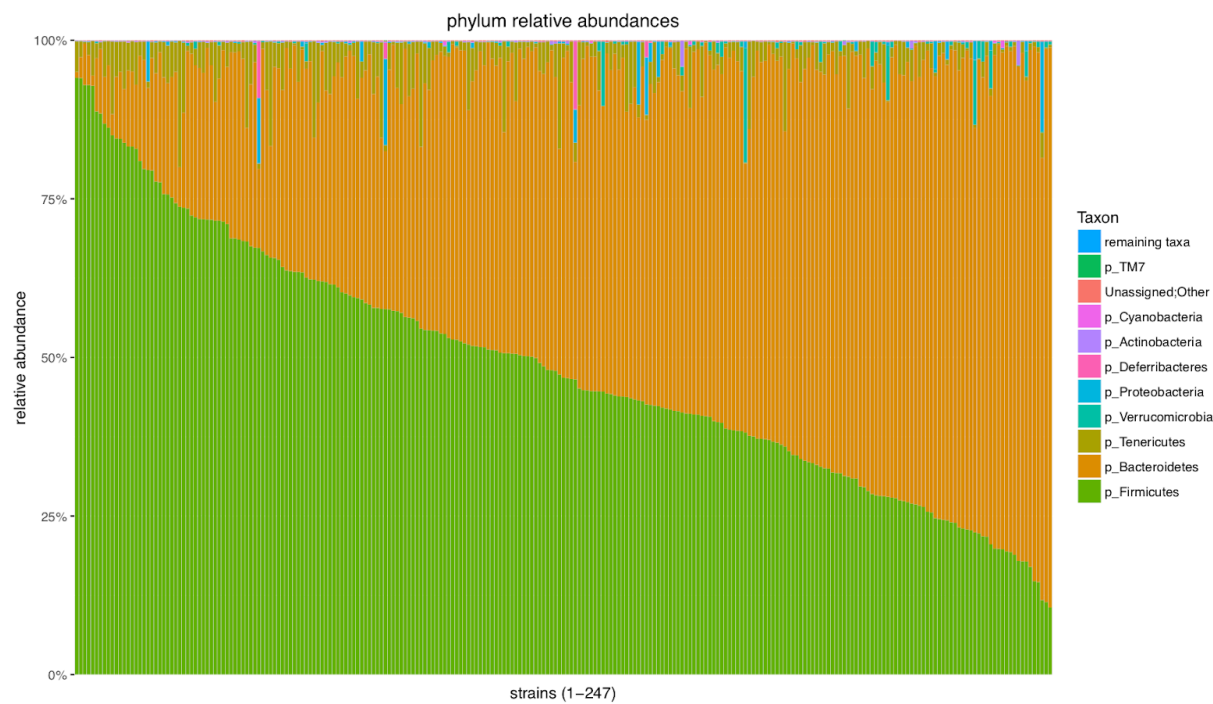


Figure S4.1 - Taxa relative abundance frequencies - Stacked bar plots and box plots depicting relative abundance frequencies of the top ten most abundant taxa for each of five taxonomic levels. Relative abundance frequencies are plotted for taxa levels from both the non-rarefied and the rarefied datasets.

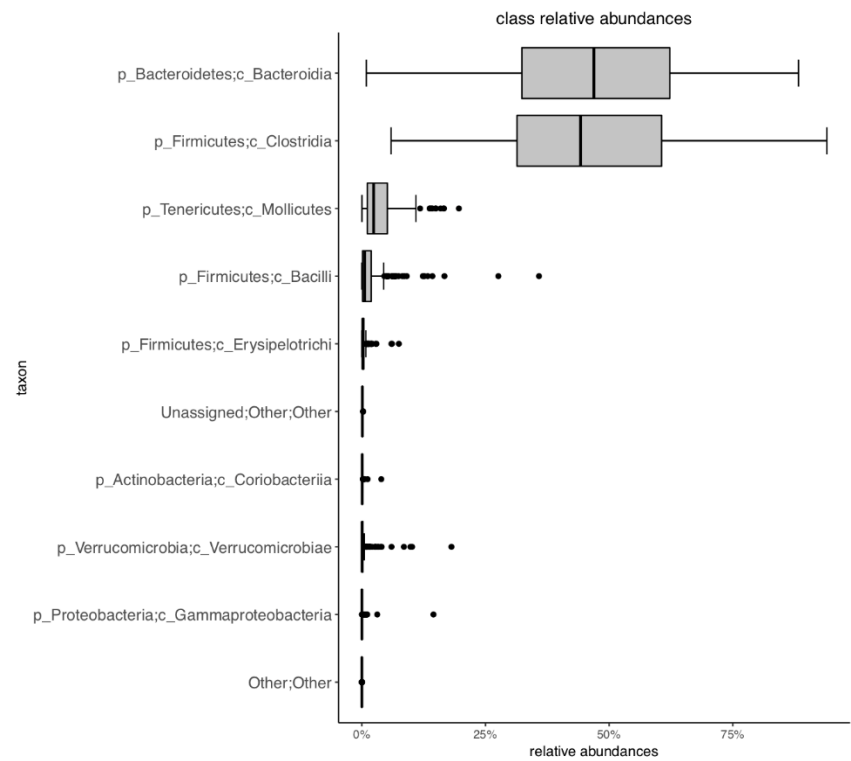
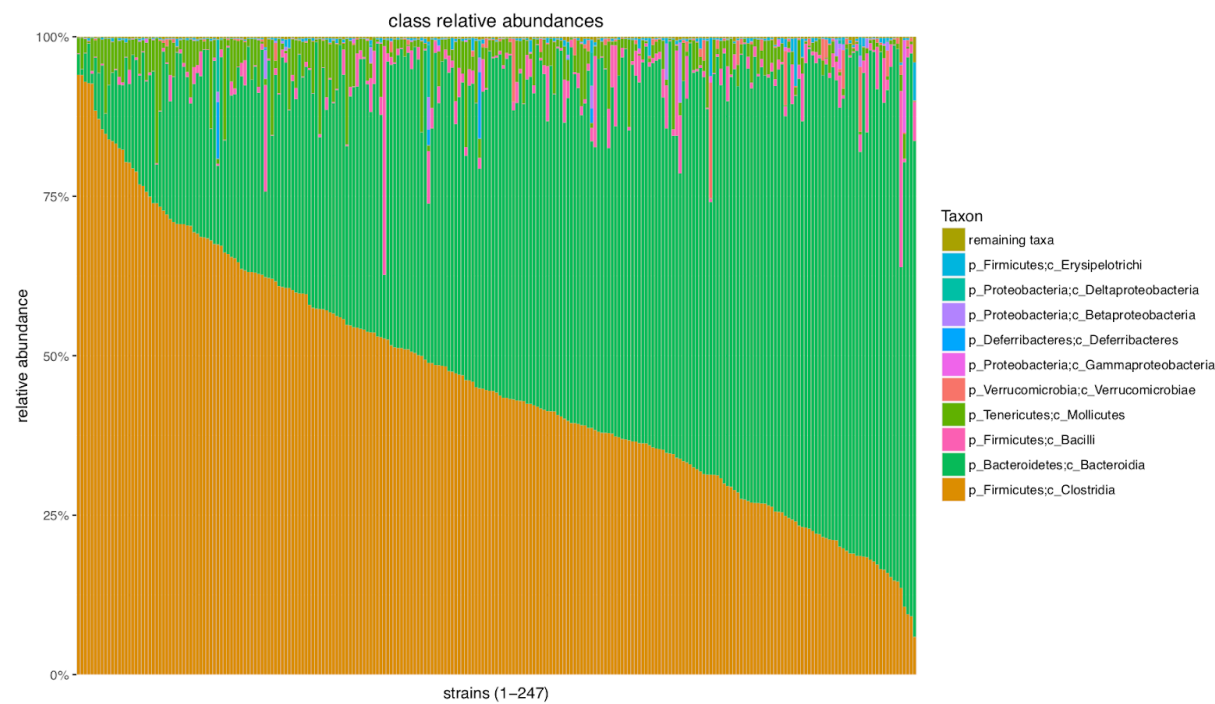
Phylum Non-Rarefied



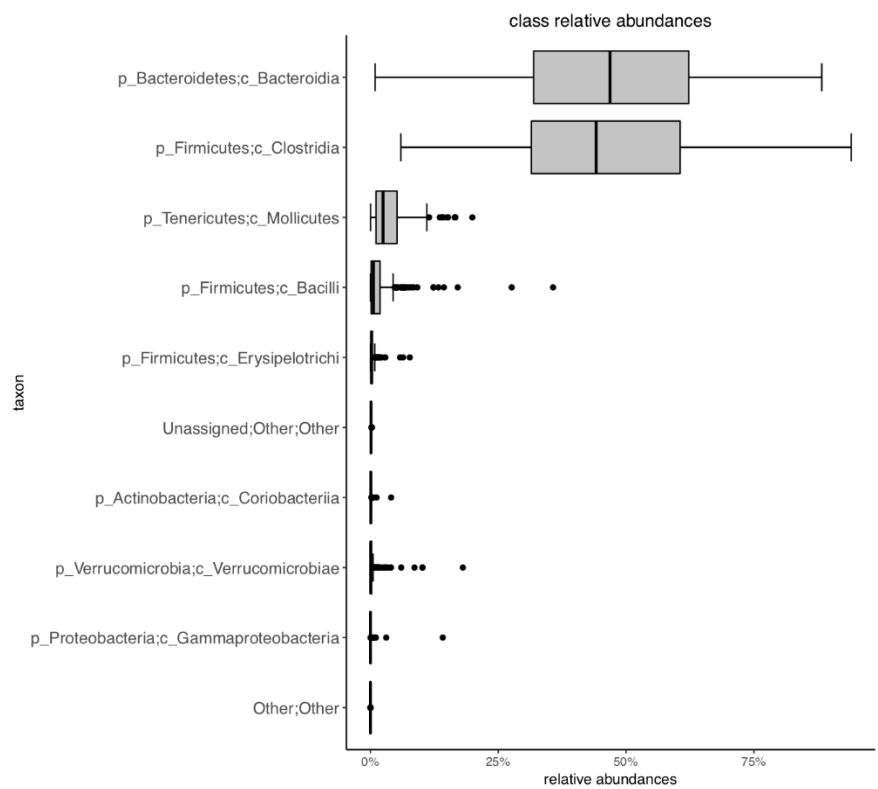
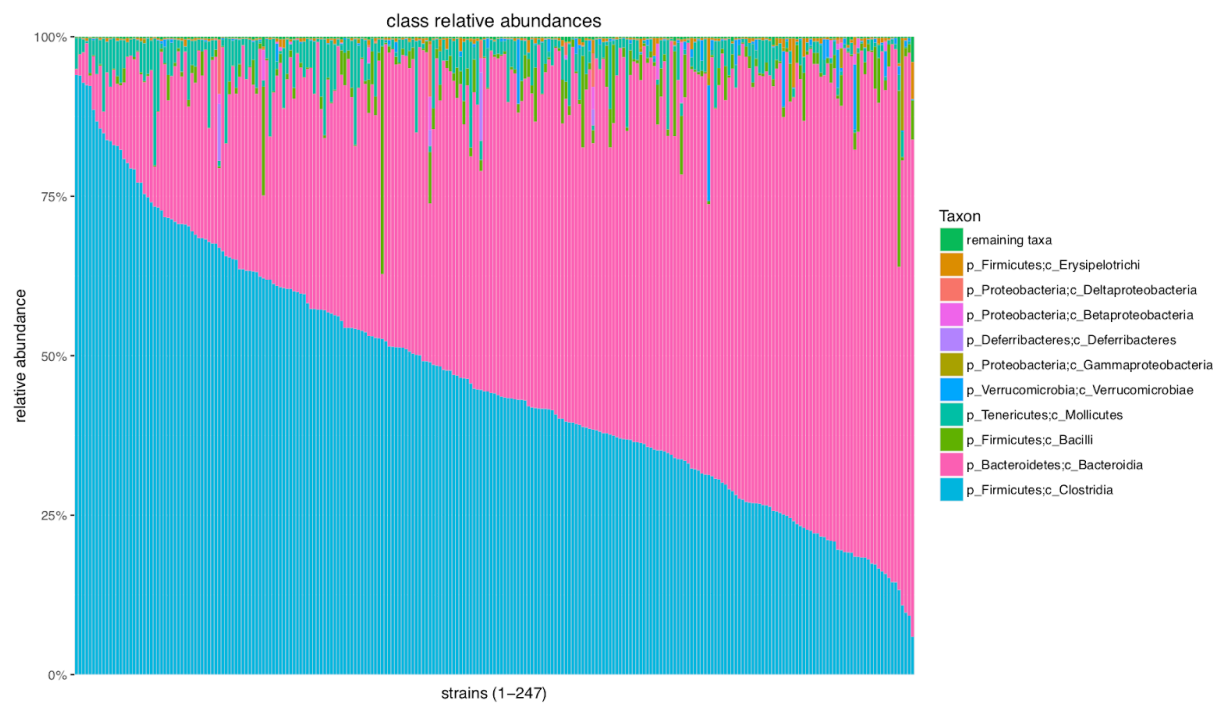
Phylum Rarefied



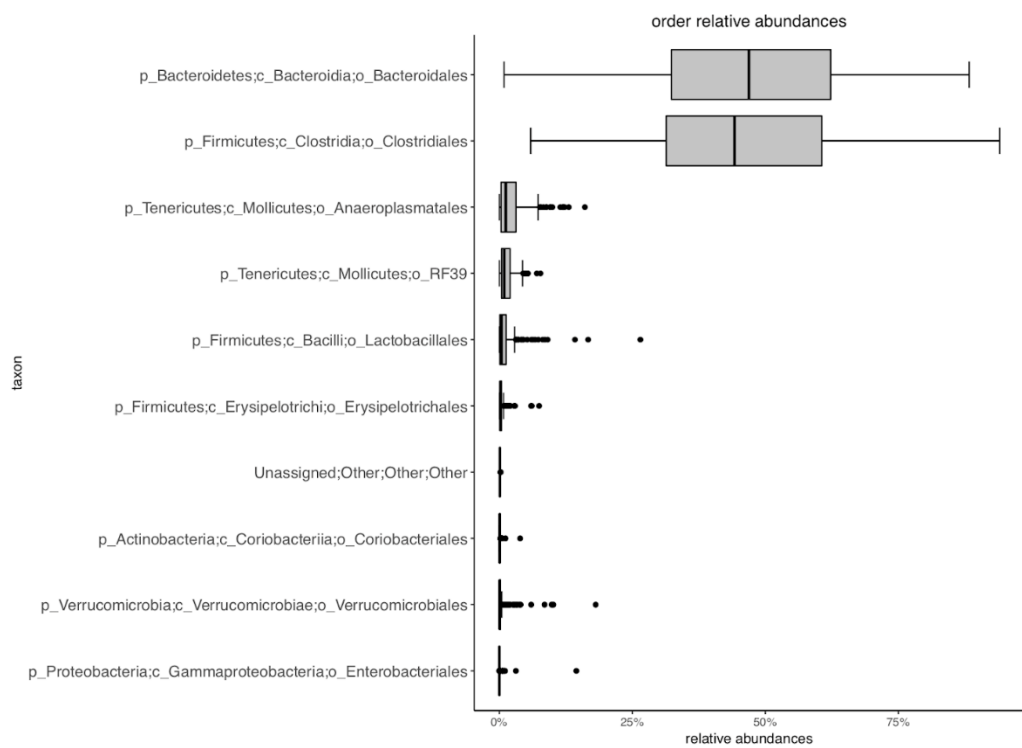
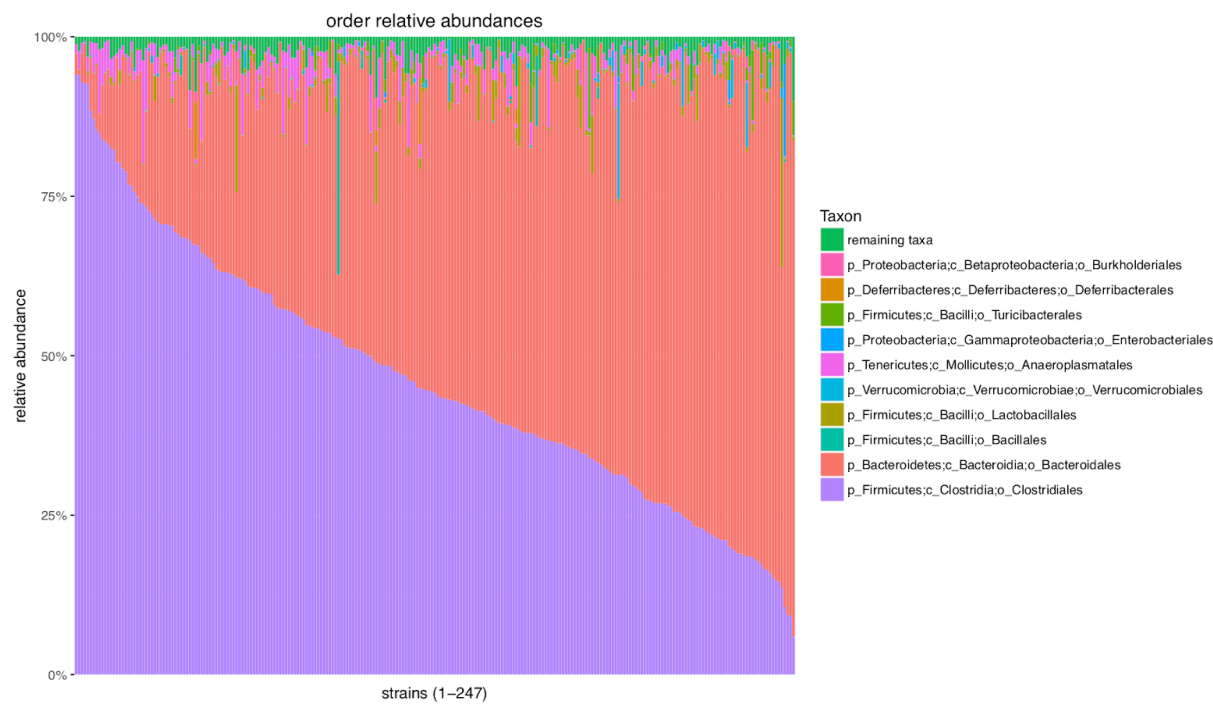
Class NonR



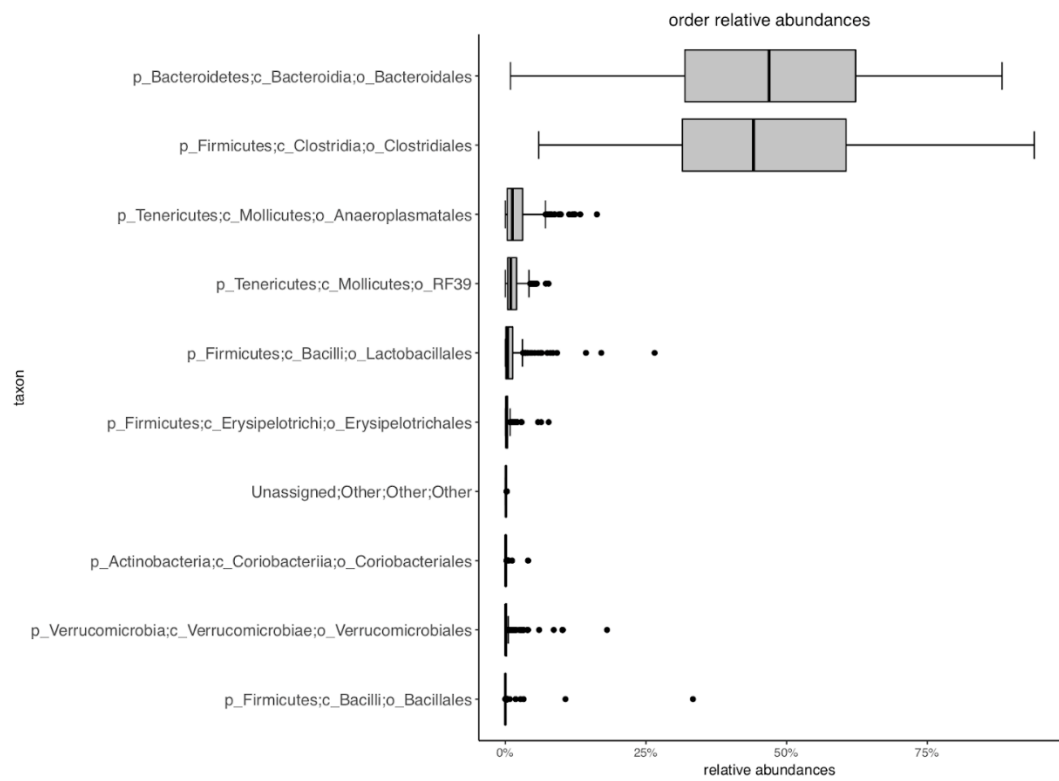
Class R



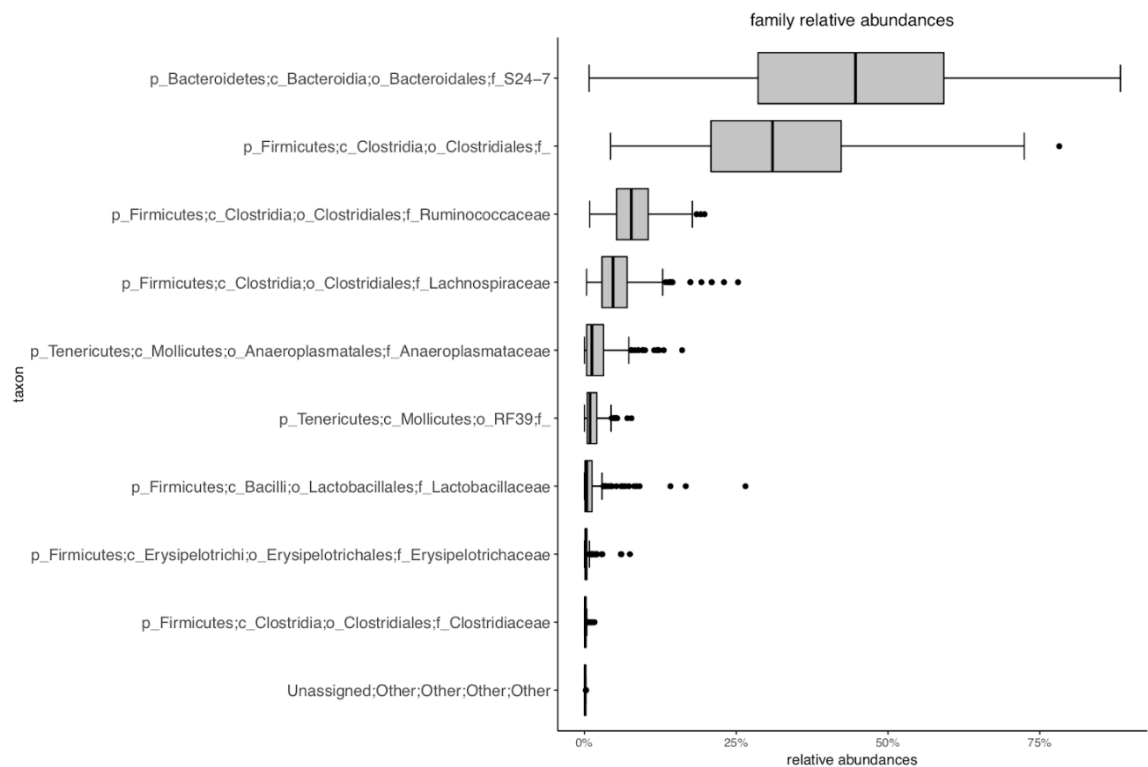
Order NonR



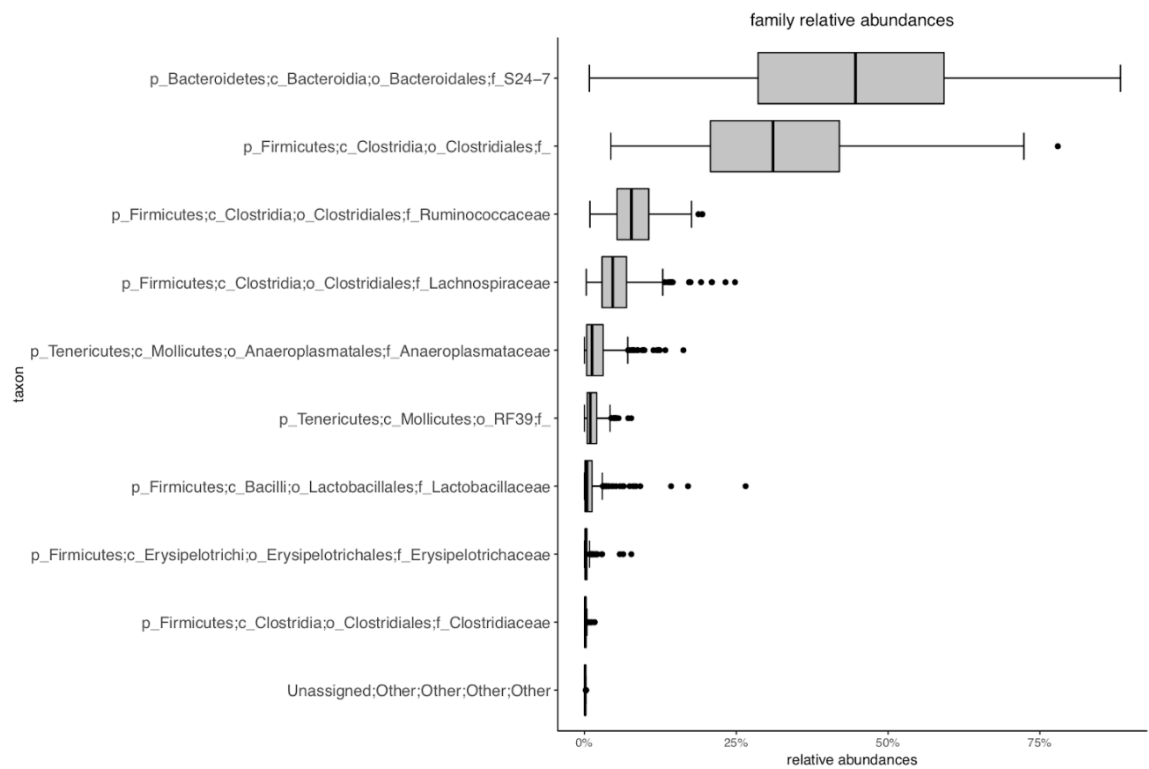
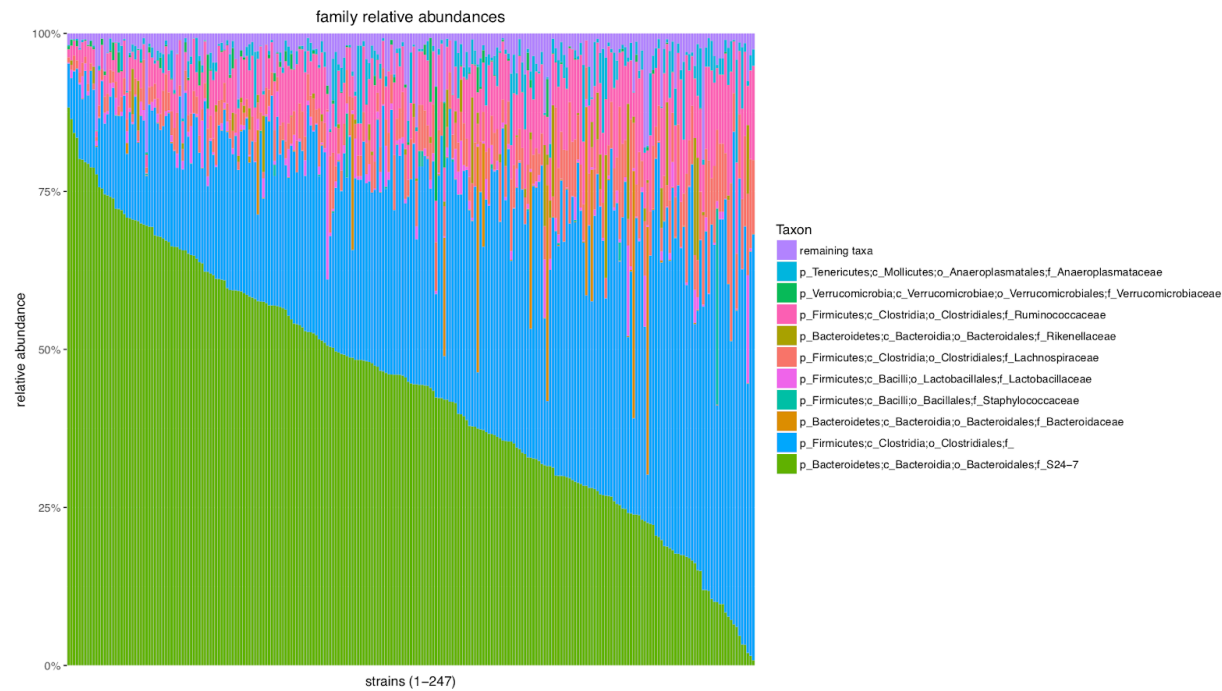
Order R



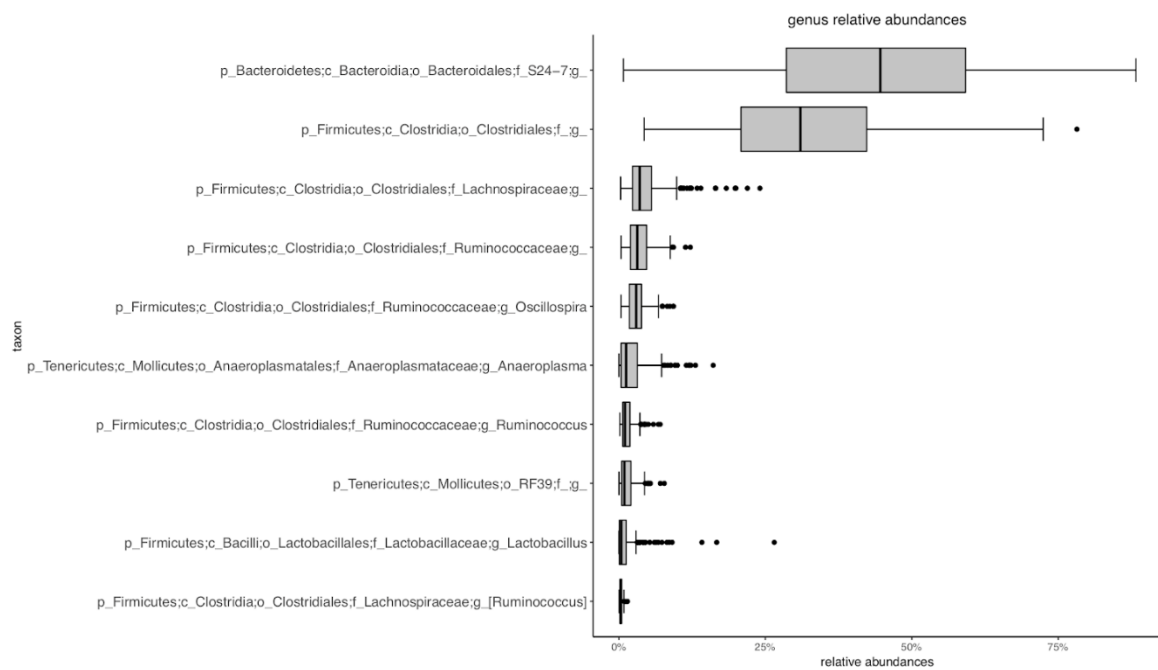
Family NonR



Family R



Genus NonR



Genus R

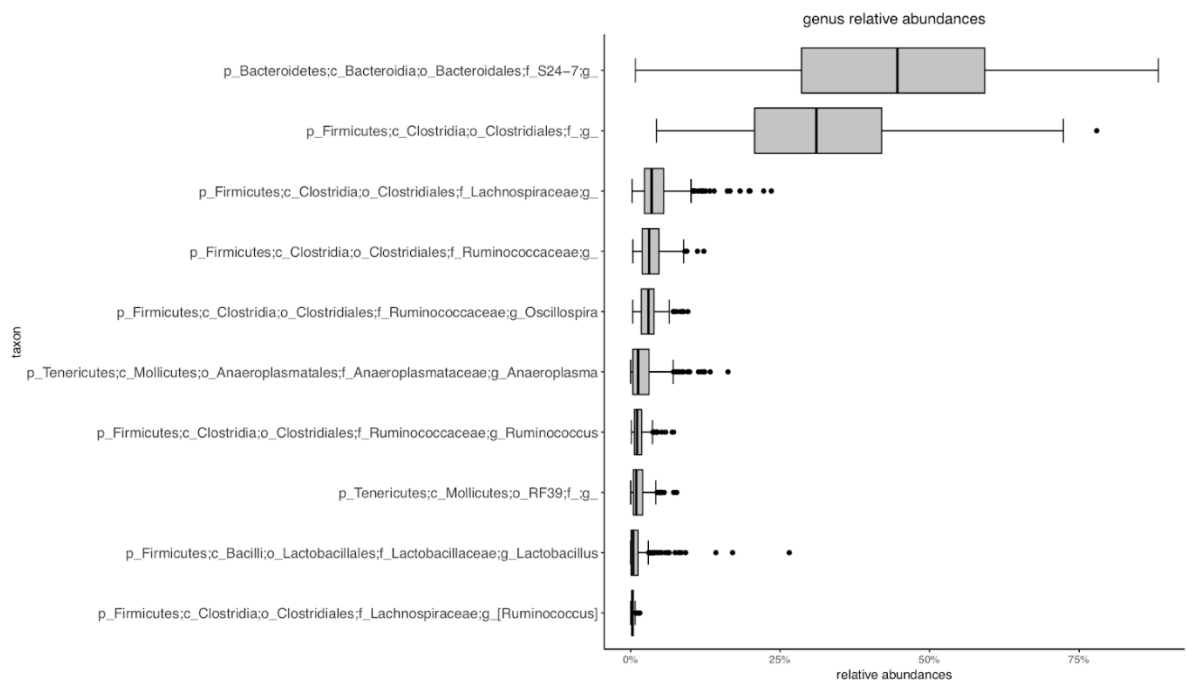
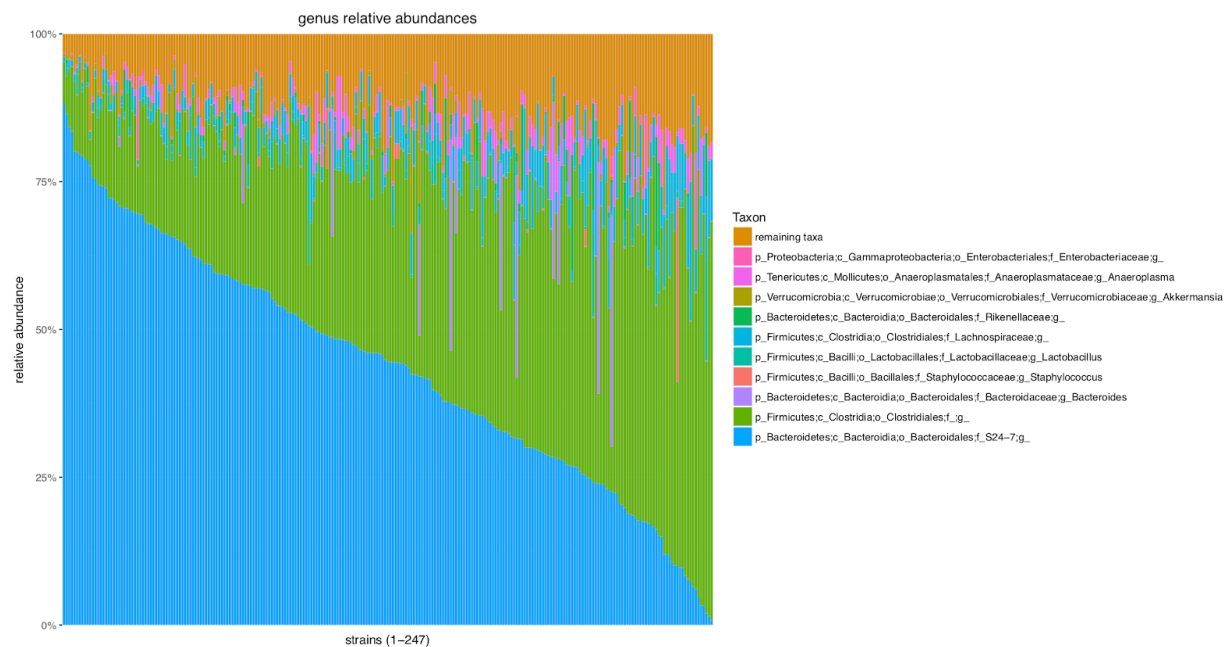


Figure S4.2 - Correlation plot between non-rarefied and rarefied taxa. Heatmap depicting the correlations between non-rarefied (NonR) and rarefied (R) taxa show that the same taxa from both non-rarefied and rarefied datasets are strongly correlated, followed by taxa belonging to the same clade.

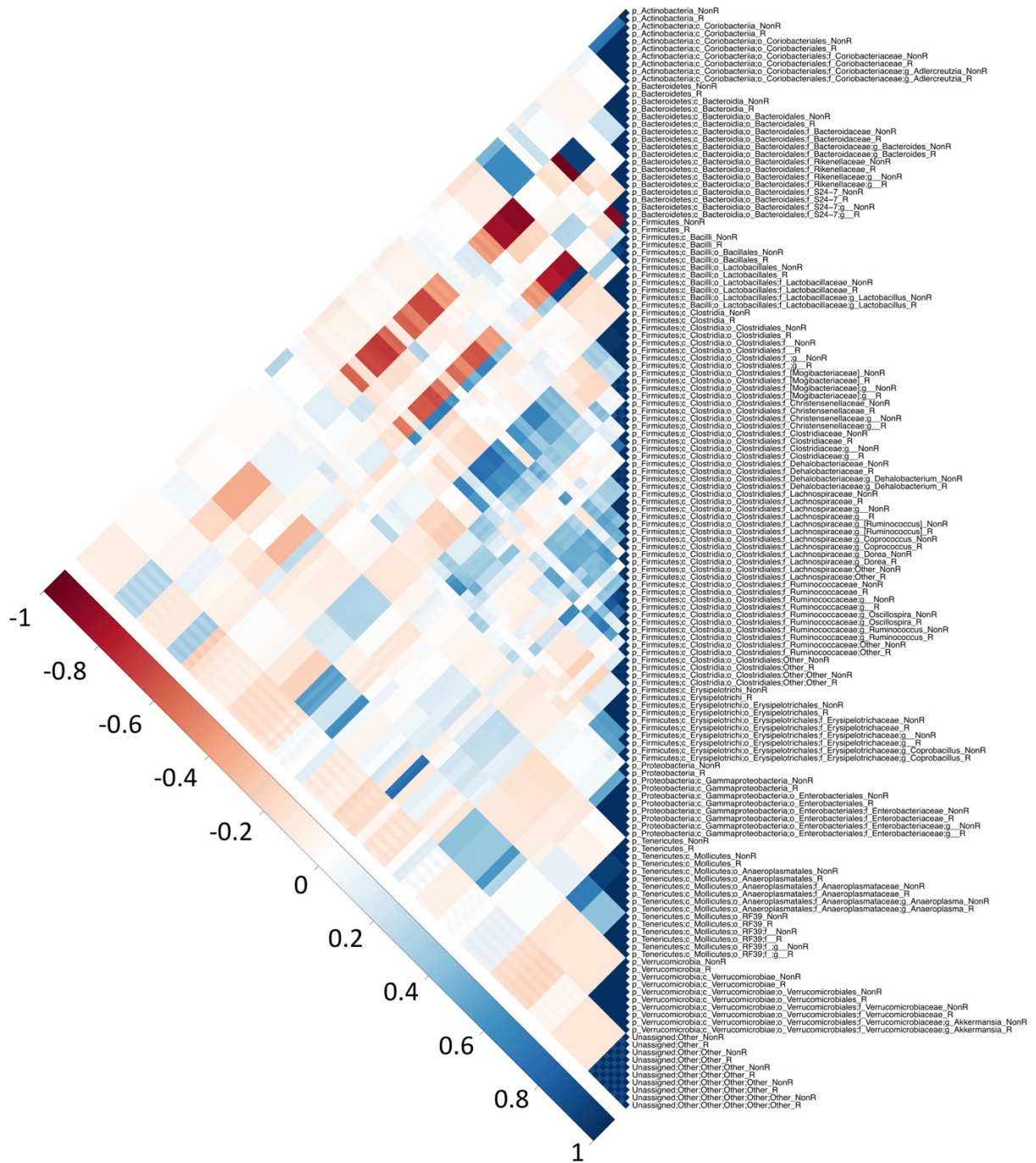


Figure S4.3 - Proportion variance estimates for kinship and cage for all OTUs. Proportion of variance for each taxon that can be explained by additive effects (heritability) using a kinship or Genomic Relationship Matrix (GRM) (green), cage effects (orange), and unexplained residual effects (blue). Taxa marked with a red asterisk have statistically suggestive QTL hits (adj. p -value < 0.1).

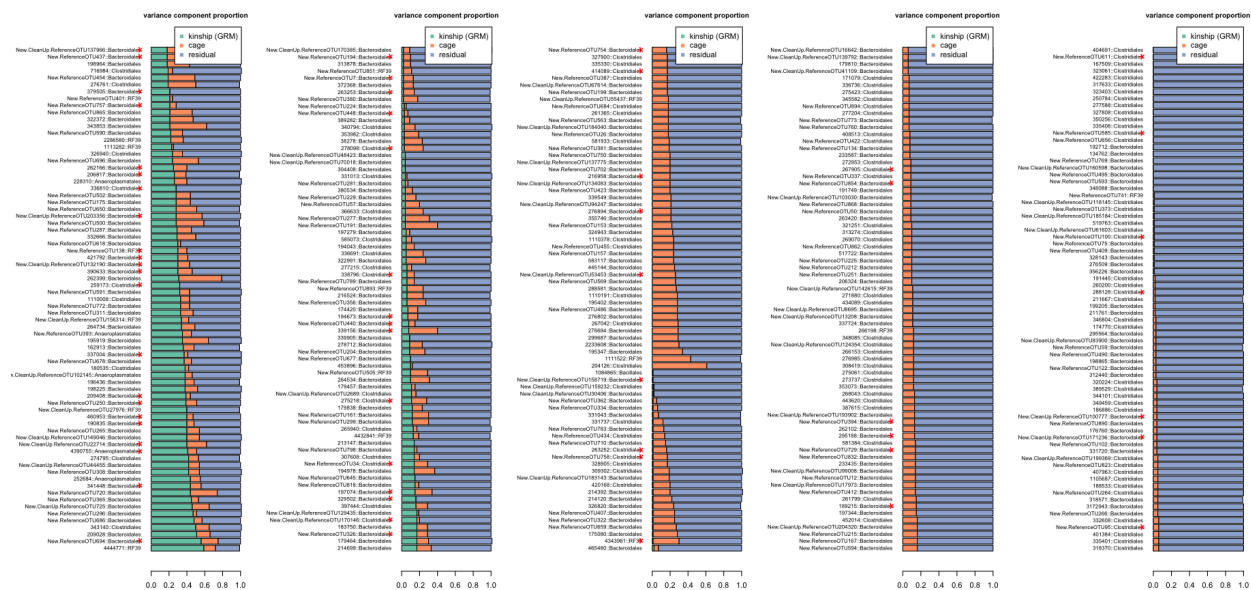
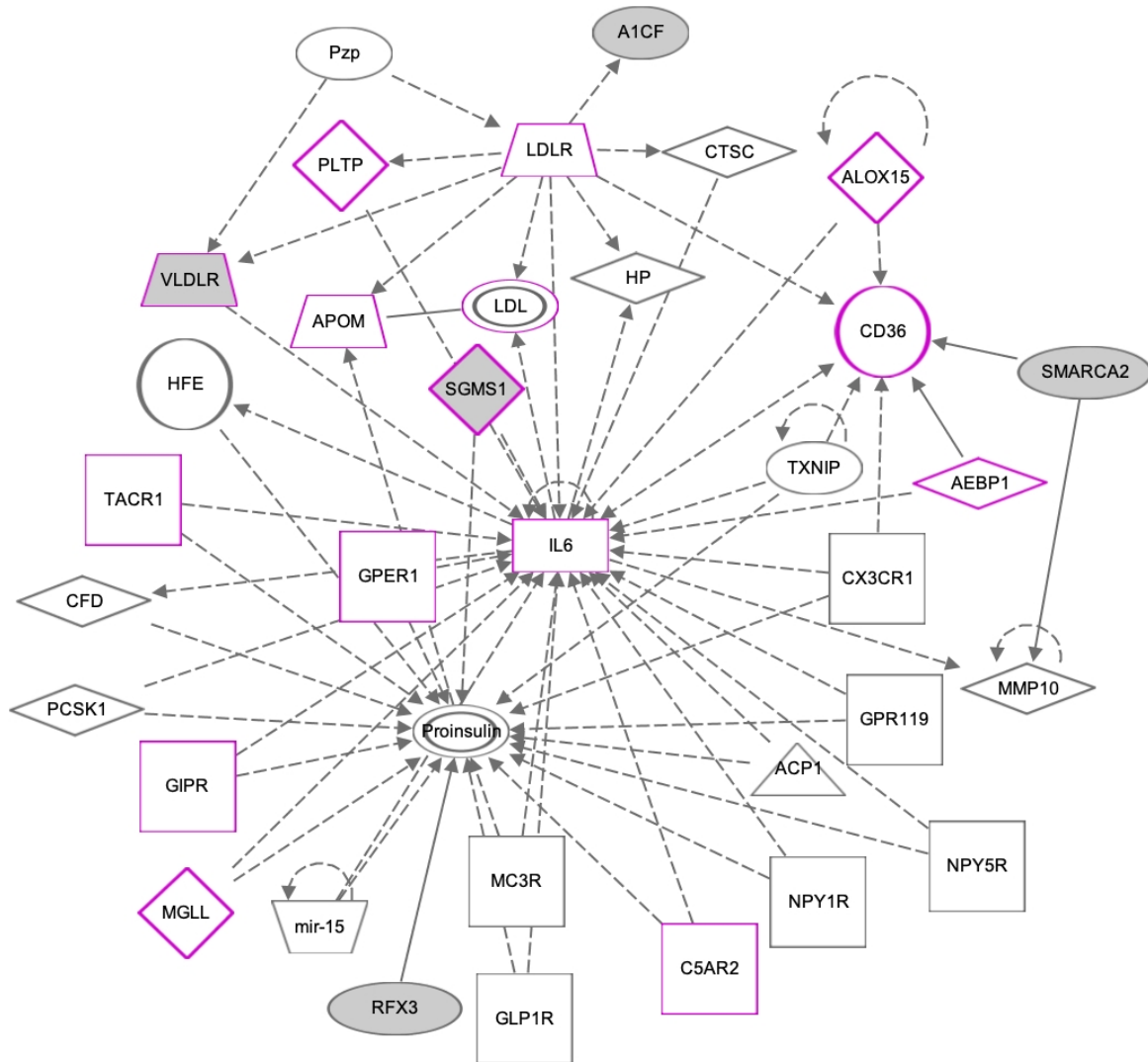


Figure S4.4 - IPA network for Bacillales QTL - Genes circled in purple are all part of the lipid metabolism pathway. Genes colored in gray belong to our dataset whereas un-colored genes are other closely associated genes added by IPA. Refer to **Tables S4.7A** for a list of these associated genes from our dataset.

Path Designer Network 1



Supplemental Material

Variation of gut microbiota in rarefied data

Samples were rarefied down to 17,410 sequences, which was the number of sequences in the sample with the least number of sequences. After keeping only the taxa present in at least 50% of samples in the rarefied dataset, we ended up with 7 phyla, 9 classes, 11 orders, 20 families, and 27 genera. Similar to the non-rarefied data, the most abundant taxa at the phylum level were Firmicutes (average relative abundance = 48.65%) and Bacteroidetes (46.39%) (**Figure S1**). The top 8 most abundant genera are present in at least 99% of the samples. The two most abundant genera were an unidentified genus within Bacteroidales family S24-7 (average relative abundance = 43.87%, ranging from 1% to 88%) and another unidentified genus within Clostridiales (32.35%, ranging from 4% to 78%) (**Figure S1**).

From our rarefied taxa, the class Mollicutes was shown to be the most highly heritable at 49% with a p -value of 0.012. All other rarefied taxa classified as statistically suggestive fall within the class of Mollicutes (unidentified genus in order RF39, and genus *Anaeroplasma*), suggesting a strong heritability pattern for Mollicutes.

Lack of effect of data rarefaction in our analysis

When dealing with uneven sequence counts across samples, microbiome studies commonly use rarefaction as a data normalization approach, consisting of randomly selecting from each sample an equal number of sequences (GOODRICH *et al.* 2014). This number is usually equal to the total sequence count of the sample with the smallest number of sequences in the dataset. It has been argued, however, that rarefaction is not an ideal approach when dealing with uneven sequence counts (MCMURDIE AND HOLMES 2014). One of the major disadvantages of this method is valuable data is being discarded. This is especially apparent when normalization attempts to treat differentially abundant taxa in an equal manner (WEISS *et al.* 2017). As an alternative to rarefaction, we decided to run our analysis on non-rarefied data, while using sequence counts per sample as a covariate. This alternative approach should increase power by retaining the full data set (MCMURDIE AND HOLMES 2014).

In order to check whether our non-rarefied dataset would give different results from using rarefaction, we estimated heritability and ran QTL mapping analysis in parallel on rarefied data and non-rarefied data. Samples were rarefied down to 17,410 sequences, which was the minimum number of reads sequenced per sample. After keeping only the taxa present in at least 50% of samples in the rarefied dataset, we ended up with 7 phyla, 9 classes, 11 orders, 20 families, and 27 genera. The most predominant taxa and their abundances in the rarefied dataset were extremely similar to that of the original non-rarefied dataset. The most abundant taxa at the phylum level were Firmicutes (average relative abundance = 48.65%) and Bacteroidetes (46.39%) (**Figure**

S1). The top 8 most abundant genera are present in at least 99% of the samples. The two most abundant genera were an unidentified genus within Bacteroidales family S24-7 (average relative abundance = 43.87%, ranging from 1% to 88%) and another unidentified genus within Clostridiales (32.35%, ranging from 4% to 78%) (**Figure S1**).

From our rarefied taxa, the class Mollicutes was shown to be the most highly heritable at 49% with a p -value of 0.012. All other rarefied taxa classified as statistically suggestive fall within the class of Mollicutes (unidentified genus in order RF39, and genus *Anaeroplasma*), suggesting a strong heritability pattern for Mollicutes.

The strong similarity between the non-rarefied and rarefied datasets is also reflected in the high Pearson correlation in the relative common taxa abundances across the two, revealing that the same taxa from both non-rarefied and rarefied datasets always group closer together than with other taxa, followed by taxa belonging to the same clade (**Figure S2**).

A concern with performing microbiome analysis is that the standard data processing method of rarefaction of counts causes notable losses of data and loss of power leading to missed associations (MCMURDIE AND HOLMES 2014). We evaluated the impact of rarefaction on microbial abundances by clustering rarefied and non-rarefied taxa together by correlation of frequency of counts within each taxonomic level. The majority of the rarefied taxa correlated with their non-rarefied counterparts (**Figure S2**). Regardless of this similarity, we conducted all analysis in parallel for non-rarefied and rarefied datasets. Looking at the significantly associated QTLs within various taxa from non-rarefied and rarefied datasets, we notice some differences in the significance of the QTLs and the chromosome in which they reside (**Table S2A-B**). While several microbial taxa associations with QTLs were consistent across non-rarefied and rarefied datasets, there were some instances of statistically significant associations being found in only one of the datasets.

Goodrich, J. K., S. C. Di Rienzi, A. C. Poole, O. Koren, W. A. Walters *et al.*, 2014 Conducting a microbiome study. *Cell* 158: 250-262.

McMurdie, P. J., and S. Holmes, 2014 Waste not, want not: why rarefying microbiome data is inadmissible. *PLOS Computational Biology* 10: e1003531.

Weiss, S., Z. Z. Xu, S. Peddada, A. Amir, K. Bittinger *et al.*, 2017 Normalization and microbial differential abundance strategies depend upon data characteristics. *Microbiome* 5: 27.